Determination of Point of Application of Tangent Force in Contact of Wheel with Drum and Its Arm Relative to Wheel Axis

M. U. Karelina[1](✉), T. A. Balabina[1], and A. N. Mamaev[2]

[1] The Moscow Automobile and Road Construction State Technical University (MADI), 64, Leningradskiy Prospect, Moscow 125319, Russia
karelinamu@mail.ru

[2] Moscow Polytechnic University, 38, Bolshaya Semyonovskaya, Moscow 107023, Russian Federation

Abstract. The evaluation of rolling resistance of automobile tires, as well as the determination of the coefficient of resistance to lateral withdrawal, is often performed on drum stands. It is also becoming increasingly common to test cars on drum stands of different designs: with different numbers of drums, their location and type of drive. This raises the problem of determining the power and kinematic characteristics of the wheel when it rolls on the drum, since these issues are not reflected in the literature. These problems can be solved, considering that the rolling mechanics of the elastic wheel on the drum is the same as when the wheel is rolling on a flat rigid support surface. In early research of the authors, general questions of the mechanics of rolling a wheel on a drum are considered in detail, considering the friction interaction of the "wheel-drum" pair. However, the question of the points of application of tangent and normal forces in contact with the drum and, accordingly, the shoulders of these forces relative to the wheel axis was not disclosed. These values are necessary, in particular, when considering the rolling of cars during tests on drum stands. In this paper, the authors derive dependencies for determining the point of application of the tangent force in contact and its shoulder relative to the wheel axis.

Keywords: Wheel · Drum · Resistance · Contact · Force · Force arm

1 Introduction

The rolling mechanics of the elastic wheel on the drum is the same as when the wheel is rolling on a flat rigid support surface [1–9].

In the papers [10–17], the equations for calculation of the power loss due to friction in the contact and hysteresis in the material of the wheel relative loss (slipping) wheel speed value were obtained under considering the mechanics of rolling elastic wheels on rigid drum. Wheel speed value is occurring in the contact tangent forces due to rolling resistance coefficient of the driven wheels. However, the question of the points of application of tangent and normal forces in contact with the drum and, accordingly,

A. A. Radionov and V. R. Gasiyarov (eds.), *Proceedings of the 6th International Conference on Industrial Engineering (ICIE 2020)*,
Lecture Notes in Mechanical Engineering, https://doi.org/10.1007/978-3-030-54814-8_10

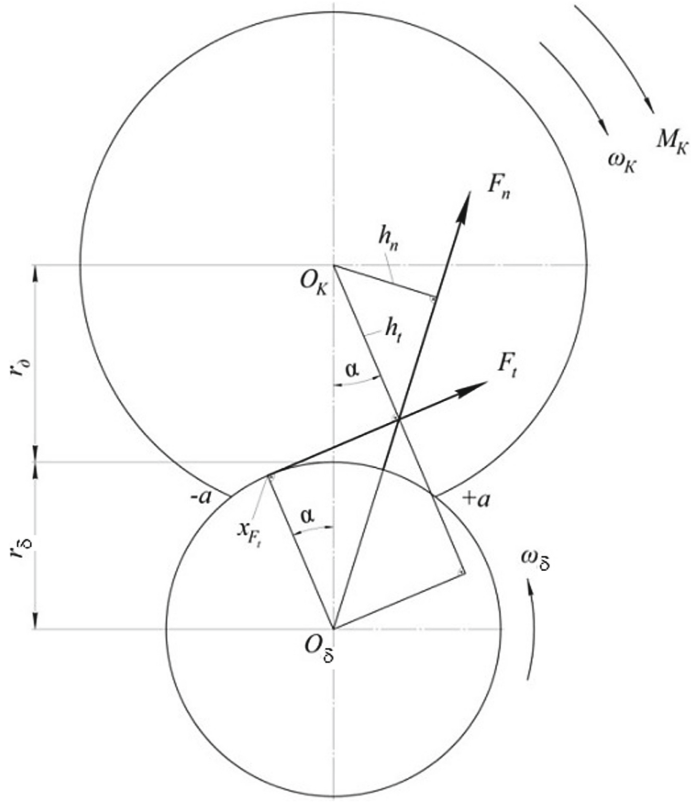

Fig. 1. Normal F_n and tangential F_t forces in the contact of the wheel with the drum

the shoulders of these forces relative to the axis of the wheel (Fig. 1). These values are necessary, in particular, when considering the rolling of cars in tests on drum stands.

This work is devoted to determining the point of application of the tangent force in contact and its shoulder relative to the axis of the wheel.

2 Main Part

The elementary tangent forces $dF_\tau = q_t dx 2b$ distributed along the arc of the wheel-drum contact have a resultant, defined as the geometric sum of the elementary tangent forces (Fig. 2), and located outside the surface of the drum.

To find the magnitude and the line of action of this force, consider two elementary sites of length dx each, located symmetrically with respect to the centerline $O_\delta O_K$ (Fig. 2) and distant from the center of contact at a distance $\pm x$. Linear elementary tangential forces realized at these sites, denote τ' and τ''. The resultant of these forces passes through the point of intersection of their lines of action, lying on the inter-axial

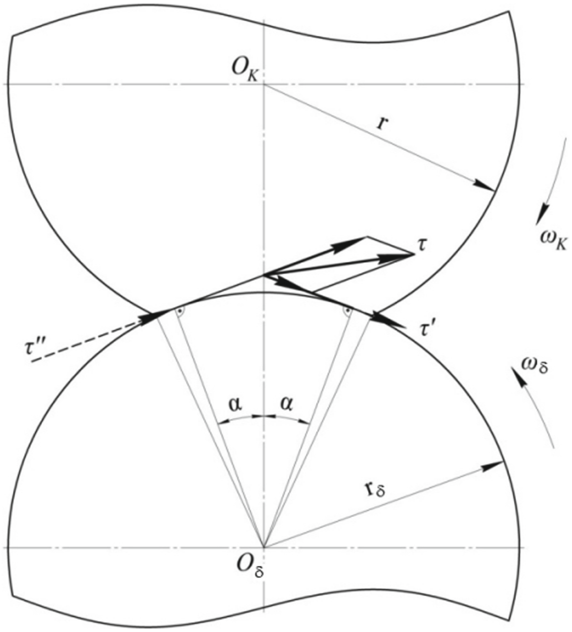

Fig. 2. Linear elementary tangential forces τ' and τ'', implemented at sites remote from the center of contact at a distance $\pm x$, and their resultant τ

line $O_\delta O_K$, and can be found by the "cosine theorem":

$$\tau = \sqrt{(\tau')^2 + (\tau'')^2 + 2\tau'\tau'' \cos 2\alpha} \tag{1}$$

where $\alpha = x/r_\delta$ is the angle that determines the position of the symmetric sites under consideration.

When the selected elementary sites are located on the coupling site, the values $\tau'^{('')}$ are determined in accordance with the equation [1, 2, 10–12, 14, 15] $\tau'^{('')} = q_t \mathrm{d}x = \lambda\xi(a - 2x)\mathrm{d}x$. If the platforms are located on the slip area, then $\tau'^{('')} = q_t^{c\kappa} \mathrm{d}x = \mu q_n \mathrm{d}x = \mu q_{n_0}\,(a^2 - x^2)\mathrm{d}x$.

Considering that $x \ll r_\delta$ and the angle α is small, the expression (1) after some transformations with power series expansion can be represented as:

$$\tau = \left(\tau' + \tau''\right)\left(1 - \frac{\tau'\tau''}{(\tau' + \tau'')^2} 2\alpha^2\right)$$

Let us consider further two cases—when the maximum traction force is realized by coupling the wheel with the drum, and when the traction force realized in contact is small.

In the first calculated case, when the traction force is realized in the contact, the linear elementary tangential forces realized on two symmetrically arranged elementary platforms of length dx are the same $\tau' = \tau'' = \mu q_n \mathrm{d}x$. Therefore, their resultant is perpendicular to the center line $O_\delta O_K$ and according to Eq. (2) it will be equal to:

$$\tau = 2\mu q_n \cos\alpha \mathrm{d}x = 2\mu q_n\left(1 - \frac{\alpha^2}{2}\right)\mathrm{d}x = 2\mu q_{n_0}(a^2 - x^2)\left(1 - \frac{x^2}{2r_\delta^2}\right)\mathrm{d}x \qquad (2)$$

The picture of the distribution of the resultant linear elementary tangent forces is presented in Fig. 3.

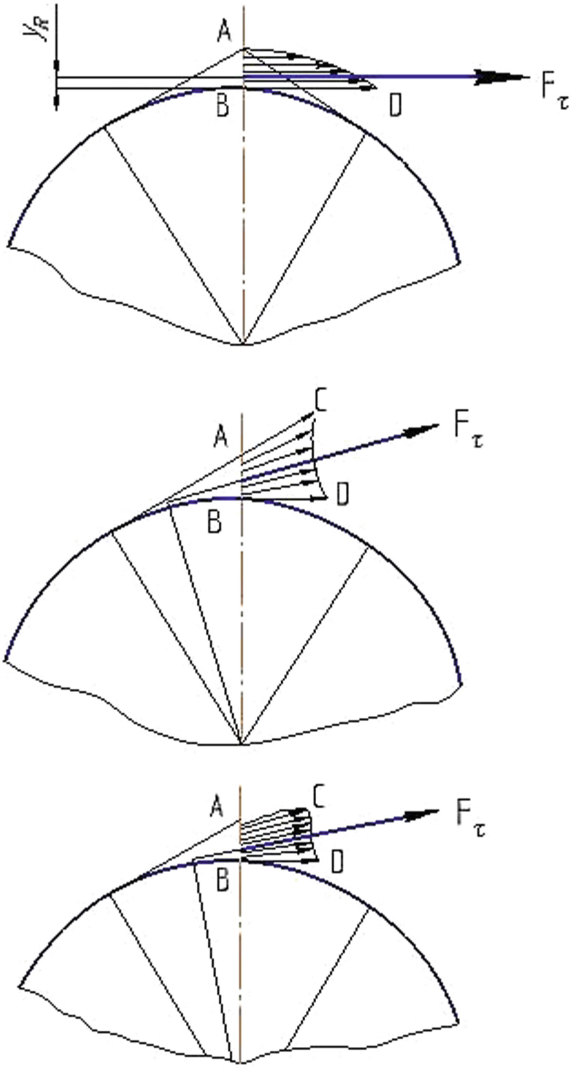

Fig. 3. Distributions of the resultant linear elementary tangent forces τ and their resultant tangent forces F_τ

The resulting tangent force is found as:

$$F_\tau = 2b\int_0^{y_0} \tau \mathrm{d}y = 4b\mu q_{n0}\int_0^{y_0}\left(a^2 - 2r_\delta y\right)\left(1 - \frac{y}{r_\delta}\right)\frac{\sqrt{yr_\delta}}{2y}\mathrm{d}y = \frac{8}{3}\mu ba^3 q_{n0}\left(1 - \frac{a^2}{10r_\delta^2}\right) \tag{3}$$

where $y = \frac{r_\delta}{\cos\alpha} - r_\delta \approx \frac{x^2}{2r_\delta}$ is the coordinate of the point of application of the elementary tangent force τ (the origin in this case is located at point B); $y_0 = a^2/2r_\delta$ corresponds to the position of point A.

According to [1, 2, 10–12, 14, 15], the circumferential thrust force equal to the algebraic sum of all specific tangent forces in contact is defined as:

$$F_t = 2b\left[\frac{\lambda\xi}{2}(a - x_S)^2 \pm \frac{1}{3}\mu q_{n0}\left(2a^3 + 3a^2 x_S - x_S^3\right)\right] \tag{4}$$

where x_S is the coordinate of the boundary of the clutch and slip areas in contact, b is the width of the contact spot.

In the implementation of the limit on the coupling of the circumferential traction force, the value of the latter is equal to $F_t = \frac{8}{3}\mu ba^3 q_{n0}$. Comparing the value of this force with the value F_τ, obtained above, it can be concluded that the resulting tangent force F_τ is less than the thrust force F_t, but their difference is so small that it can be neglected.

The line of action of the tangent force F_τ is perpendicular to the center line $O_\delta O_K$ and is located (Fig. 4a) above the circumference of the drum: $\frac{AB}{2} = \frac{a^2}{4r_\delta} > y_R > \frac{AB}{3} = \frac{a^2}{6r_\delta}$.

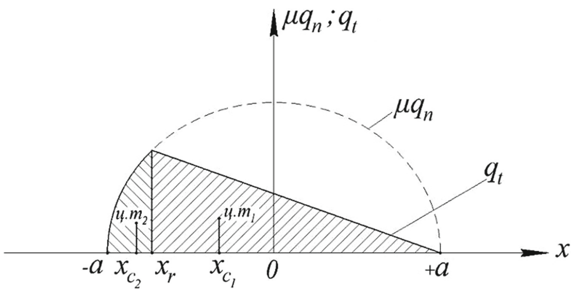

Fig. 4. Plots of longitudinal tangential stresses q_t and normal pressures q_n in the longitudinal section of the contact spot; coordinates of the centers of gravity of the tangential stresses plot

In the second case, at low thrust, the area of sliding contact is small and the coordinate boundaries of the grip and slide close to $x = -a$. So, to simplify, it is assumed that the plot of the distribution of tangential stress along the entire length of the contact patch takes the triangle shape. As a result, considering in this case x as an arithmetic quantity, we get:

$$t' = \lambda\xi(a - x)d \quad t'' = \lambda\xi(a + x)\mathrm{d}x$$

$$\tau = 2\lambda\xi a\left(1 - \frac{a^2 - x^2}{2a^2 r_\delta^2}x^2\right)\mathrm{d}x$$

The picture of distribution τ, constructed by the last equation, is presented in Fig. 3b. The lengths of the vectors $A\bar{C} = \bar{\tau}''$ and $B\bar{D} = \bar{\tau}'$ for x equal to $x = a$ and $x = 0$ are the same. In view of the smallness of the second term in parentheses of the last equation with a sufficient degree of accuracy, it can be assumed that the vector of the resulting tangent force F_τ of the system of forces τ passes through the middle of the segments AB and CD, and the modulus of force is equal to:

$$F_\tau = 2b\int_0^{y_0} \tau\sqrt{2\left(1 + \cos\frac{\alpha_0}{2}\right)}\mathrm{d}y \approx 2b\int_0^{y_0} 2\tau\left(1 - \alpha_0^2/16\right)\mathrm{d}y = 4ba^2\left(1 - \frac{a^2}{16r_\delta^2}\right)\lambda\xi. \tag{5}$$

where, as in the previous case, $y = \frac{r_\delta}{\cos\alpha} - r_\delta \approx \frac{x^2}{2r_\delta}$. is the coordinate of the point of application of the elementary tangent force τ (the origin in this case is also located at point B).

Considering the assumed smallness of the thrust force and $x_S = -a$ from the formula (4), which determines the magnitude of the thrust force, we obtain $F_t = 4ba^2\lambda\xi$. Comparing the last expression with the dependency for F_τ, it can be written as:

$$F_\tau = F_t\left(1 - \frac{a^2}{15r_\delta^2}\right)^2,$$

i.e. the tangential force, which acts from the side of the drum on the wheel, is the resultant of elementary tangential forces, which is less than the circumferential thrust force realized in contact; however, this difference is very small, and it can practically be neglected.

From the equality of the moments produced by forces F_t and F_τ, $M_t = F_t\ r_\delta = F_\delta\ r_\delta$, get the shoulder action of the resultant of the tangential forces F_τ equal to $r_\tau = r_\delta\ F_t/F_\tau$. Despite of the shoulder exceeds the value of r_τ and the value of r_δ, and the difference between these values is very small, and it can be considered that $r_\tau \approx r_\delta$.

The angle of inclination F_τ at low thrust forces is approximately $\varphi \approx \alpha_0/2$, which corresponds to $x_{F\tau} \approx -a/2$.

It should be noted that if we consider the difference $x_S \neq -a$, the picture of the distribution of the resultant elementary tangent forces will change slightly in the area of point A (Fig. 3b) and the total resultant tangent force will be located slightly lower than previously accepted, and with a smaller angle of inclination.

With the growth, which is realized in contact with the thrust force F_t, tangential force F_τ falls, as expected, below the angle between the center line $O_\delta O_K$ and the line of action of F_τ. This angle will be closer to 90°. The coordinate $x_{F\tau}$, determines the angle $\alpha_\tau = x_{F\tau}/r_\delta$, the slope of the line of action of this force will change from $x_{F\tau} = -a/2$ to $x_{F\tau} \to 0$.

In further calculations, as already shown, we can assume that $F_t = F_\tau$, and the coordinate $x_{F\tau}$ to take equal to $x_{F\tau} \approx -0.5a$.

However, given that, $x_{F\tau}$ still depends on the realized thrust force, it is desirable to obtain an analytical dependence $x_{F\tau} = f(F_t)$.

At $a \ll r_\delta$, the elementary tangential forces $q_t 2bdx$, as well as the tangential stresses q_t, can be conditionally considered acting in one direction due to the smallness of the angles α of their inclination.

Consider the plot of tangential stresses (Fig. 4), the area of is numerically equal to the linear thrust force $F_t/2b$.

The coordinate of the center of gravity of this plot can be considered the point of application of the thrust force and, under accepted conventions, the point of application of the resulting tangent force.

The plot can be divided into two figures, one of which corresponds to the tangential stresses on the clutch section, and the other to the tangential stresses on the slip section.

It is known that the coordinate of the center of gravity of the figure is calculated as:

$$x_c = \frac{\int_{x_1}^{x_2} xy\mathrm{d}x}{A}, \tag{6}$$

where A is the area of the figure; y is its current ordinate; x_1 and x_2 are the coordinates of the figure boundary.

For the first figure

$$y = q_{t_x} = \lambda\xi(a - x); \quad x_1 = x_S; \quad x_2 = +a;$$

$$A_1 = \int_{x_S}^{+a} q_{t_x}\mathrm{d}x = \lambda\xi(a - x_S)^2/2$$

For the second figure, $y = \mu q_n$; $x_1 = -a$; $x_2 = x_S$

$$A_2 = \int_{-a}^{x_S} \mu q_n \mathrm{d}x$$

Then,

$$x_{c_1} = \frac{\int_{x_S}^{+a} x\lambda\xi(a - x)\mathrm{d}x}{\int_{x_S}^{+a} \lambda\xi(a - x)\mathrm{d}x}; \quad x_{c_2} = \frac{\int_{-a}^{x_S} x\mu q_n \mathrm{d}x}{\int_{-a}^{x_S} \mu q_n \mathrm{d}x}$$

The coordinate of the center of gravity of the entire figure can be found as:

$$x_{F_t} = \frac{\sum A_i x_{c_i}}{\sum A_i}$$

or, substituting the previous expressions:

$$x_{F_t} = \frac{A_1 x_{c_1} + A_2 x_{c_2}}{A_1 + A_2} = \frac{\int_{-a}^{x_S} x\mu q_n \mathrm{d}x + \int_{x_S}^{+a} x\lambda\xi(a - x)\mathrm{d}x}{\int_{-a}^{x_S} \mu q_n \mathrm{d}x + \int_{x_S}^{+a} \lambda\xi(a - x)\mathrm{d}x}$$

After the transformations, considering that the expression in the denominator is the linear thrust force $F_t/2b$ [10–12, 14, 15], we obtain:

$$x_{F_t} = -\frac{\mu q_{n_0} b}{6F_t}\left(a^2 - x_s^2\right), \tag{7}$$

If to substitute the expression received earlier [10–12, 14] to the last equation

$$x_s = a\left(1 - 2\sqrt[3]{1 - \frac{F_t}{\mu F_z}}\right)$$

we will finally get:

$$x_{F_t} = a\left(1 - \frac{\mu F_z}{F_t}\right)\left(1 - \sqrt[3]{1 - \frac{F_t}{\mu F_z}}\right) \tag{8}$$

For small tangent forces compared to the coupling limit, the dependence (8) can be represented in a simplified form if decomposed $\sqrt[3]{1 - \frac{F_t}{\mu F_z}}$ into a power series:

$$x_{F_t} = a\left(1 - \frac{\mu F_z}{F_t}\right)\frac{F_t}{3\mu F_z} = \frac{a}{3}\left(\frac{F_t}{\mu F_z} - 1\right) \tag{9}$$

In the expressions (8) and (9), the value of the F_t force is taken modulo.

From the dependencies obtained for $x_{F\tau}$, it can be seen that for $F_t \to \mu F_z$ $x_{F_t} \to 0$;

•pЏ $F_t = \frac{7}{8}\mu F_z$ $x_{F_t} \approx -0.07a$; •pЏ $F_t = \frac{1}{2}\mu F_z$

$x_{F_t} \approx -0.2a$; •pЏ $F_t = 0.25\mu F_z$ $x_{F_t} \approx -0.25a$; •pЏ $F_t = 0.125\mu F_z$

$x_{F_t} \approx -0.3a$; •pЏ $F_t \to 0$ $x_{F_t} \to -0.33a$

The shoulder of the action of the tangent force relative to the center of the wheel is for geometric reasons:

$$h_\tau = O_\delta O_k \cos\alpha_\tau - r_\delta = (r_d + r_\delta)\cos\alpha_\tau - r_\delta \tag{10}$$

where angle is

$$\alpha_\tau = x_{F_\tau}/r_\delta \tag{11}$$

after the transformations, we get

$$h_\tau = r_d\left(1 - x_{F_\tau}^2/2r_d r_\delta\right) \tag{12}$$

3 Conclusion

The equations for determining the point of application of the tangent force in contact and its shoulder relative to the wheel axis are derived from the consideration of the mechanics of interaction between an elastic wheel and a drum. These dependencies have a simple form and can be applied when considering the rolling of a car on a drum stand. The study of the roller wheel with a tilt of the wheel and the influence of the bulge of the treadmill of the wheel is given in the works [17–28].

References

1. Vyrabov RV, Mamaev AN (1980) Analysis of kinematic and power relations when rolling an elastic wheel on a rigid base. Mech Mach 57:101–106
2. Vyrabov RV, Mamaev AN (1978) Determination of the power of friction losses in the contact of a friction pair of wheels with a pneumatic tire-a rigid base. Stepless-Adjustable Trans Inter-Univ Collect Sci Yaroslavl 3:61–67
3. Vyrabov RV, Mamaev AN, Balabina TA (2010) General issues of the interaction of the elastic wheel with a rigid support surface. In: Materials of International scientific-practical conference of the Association of Automotive Engineers (AAI), Automobile and tractor industry in Russia development priorities and training dedicated to the 145th anniversary of MGTU MAMI, Izd NAMI, pp 73–80
4. Balabina TA, Mamaev AN (2014) Mechanics of rolling an elastic track on a rigid support surface. In: Collection Technical Sciences trends prospects and technologies of development, pp 20–25
5. Mamaev AN (1982) Determination of the coefficient of tangent elasticity of a wheel with a toroidal shape of a treadmill. WPI Univ Mech Eng 10
6. Vyrabov RV, Mamaev AN (1987) On the question of the lowest value of the rolling resistance coefficient of an elastic wheel on a rigid horizontal surface. WPI Univ Mech Eng 10:85–88
7. Yermilov VN, Mamaev AN (1982) Experimental investigation of stresses in the contact of a massive rubber tire and a rigid base during rectilinear rolling of the wheel. Proc Tires Rubber-Tech Asbestos-Tech Prod 6:31–33
8. Ermilow VN, Mamaev AN (1983) Experimental study of the contact stresses between a solid rubber tire and a rigid surface during rolling of the wheel in a straight-line. Int Polymer Sci Technol 107:78–79
9. Mamaev AN, Alepin EA (1980) Determining the size of the contact area and deflection of the wheel with a rubber tire when the wheel is statically pressed against a rigid base. Collect Sci Works Mach Sci 251:82–85
10. Mamaev AN et al (2010) Determination of power and kinematic characteristics of an elastic wheel when rolling on a rigid drum. In: Proceedings of the international scientific conference dedicated to the 145th anniversary of MSTU MAMI, Moscow
11. Mamaev AN, Balabina TA, Gaevskiy VV (2019) Mechanics of wheel interaction with a drum in SB. Safety of wheeled vehicles under operating conditions. In: Materials of the 106th International scientific and technical conference, pp 333–345
12. Mamaev AN (2010) Rolling resistance of the driven co-scaffold on a rigid drum. In: Proceeding of the international scientific conference dedicated to the 145th anniversary of MSTU MAMI, Moscow
13. Abuzov VI, Mamaev AN (2012) Rolling of an elastic wheel on two rigid drums. Automob. Ind. 10:19
14. Mamaev AN, Balabina TA, Odinokova IV, Gaevskiy VV (2019) Interaction mechanics of the wheel with the drum. In: IOP conference series: materials science and engineering, 632(1)
15. Karelina MYu, Balabina TA, Mamaev AN (2020) Mechanics of elastic wheel rolling on rigid drum. In: ICIE Proceedings of the 5th international conference on industrial engineering (ICIE 2019), pp 531–540
16. Mamaev AN, Balabina TA, Gaevskiy VV (2019) Mechanics of wheel-drum interaction in the collection safety of wheeled vehicles in use. In: Materials of the 106th International scientific and technical conference, pp 333–345
17. Mamaev AN, Vladimirov VN (2000) Influence of the corners of elastic wheels on rolling resistance. In: International scientific symposium devoted to the 60th anniversary of MAMI's recreation, Moscow

18. Vyrabov RV, Mamaev AN, Marinkin AP, Yuriev YuM (1986) Influence of the rolling mode of an elastic wheel on the value of the lateral force during lateral withdrawal. Vestnik Mashinostroeniya 1:33–35
19. Balabina TA, Mamaev AN, Chepurnoy SI (2013) Determination of the ratio of camber angles and convergence of elastic wheels which provides the least resistance to rolling. WPI MAMI MSTU 1(15):32–37
20. Vyrabov RV, Mamaev AN (1980) Analysis of force correlations during rolling of a driven elastic cylindrical wheel along a curved trajectory. Mech Mach 57:105–112
21. Vyrabov RV, Mamaev AN (1980) Investigation of contact phenomena in curved rolling of a toroidal wheel. WPI Mashinostroenie 2:33–38
22. Vyrabov RV, Mamaev AN (1980) Determination of forces and moments acting on the toroidal wheel in nonlinear rolling. WPI Univ Mech Eng 3:30–34
23. Mamaev AN, Sazanov IV, Nazarov YuP (1990) Determining the power characteristics of an elastic wheel when rolling with a deflection along a curved trajectory. In: Materials of the II all-union symposium problems of tires and rubber materials strength and durability
24. Vyrabov RV, Mamaev AN (1983) Influence of toroidal elastic wheel on the unevenness of its wear along the width of the treadmill. WPI Univ Mech Eng 9:94–97
25. Mamaev AN (1989) Features of rolling with the withdrawal of elastic toroidal wheels. In: First all-union conference problems of tires and rubber-cord composites, pp 22–28
26. Virabow RV, Mamaev AN, Dobromirov VN, Markov JL (1991) The influence of the angle setting of elastic wheels on the wear of their treads. In: Proceedings of the international symposium on the tribology of Friction materials II, pp 176–181
27. Balabina TA, Brovkina YuI, Mamaev AN (2018) Rolling with the withdrawal of elastic toroidal wheels. In: Engineering proceedings of the IV international scientific and technical conference, pp 112–116
28. Balabina TA, Brovkina YI, Mamaev AN (2019) Elastic toroidal wheel rolling with sideslip. Lecture notes in mechanical engineering, pp 2027–2035